Cell Adhesion

International Edition: DOI: 10.1002/anie.201500397
German Edition: DOI: 10.1002/ange.201500397

Molecular Encryption and Reconfiguration for Remodeling of Dynamic Hydrogels**

*Shihui Li, Erin R. Gaddes, Niancao Chen, and Yong Wang**

Abstract: *Dynamic materials have been widely studied for regulation of cell adhesion that is important to a variety of biological and biomedical applications. These materials can undergo changes mainly through one of the two mechanisms: ligand release in response to chemical, physical, or biological stimuli, and ligand burial in response to mechanical stretching or the change of electrical potential. This study demonstrates an encrypted ligand and a new hydrogel that are capable of inducing and inhibiting cell adhesion, which is controlled by molecular reconfiguration. The ligand initially exhibits an inert state; it can be reconfigured into active and inert states by using unblocking and recovering molecules in physiological conditions. Since molecular reconfiguration does not require the release of the ligand from the hydrogels, inhibiting and inducing cell adhesion on the hydrogels can be repeated for multiple cycles.*

Materials with the ability to mimic the dynamic nature of biological systems have been widely studied for the regulation of cell adhesion, because cell adhesion is important to various applications, such as regenerative medicine, clinical diagnoses, and cellular biology.[1,2] Most of these materials display active cell adhesion ligands for initial cell adhesion, whereas they are able to release the ligands and the cells in response to a physical, chemical, or biological stimulus through the cleavage of chemical bonds or molecules.[1] For instance, light has been successfully applied to break the C–O bond linking the RGD peptide and the hydrogel network for controlling RGD density of the hydrogel to regulate cell adhesion.[1d] However, the released ligands can bind to cells owing to their high affinities, which may change intracellular signaling pathways or even induce the death of cells.[3] Thus, it would be desirable not to release the ligands from dynamic materials to ensure the intact properties of the cells. To address this issue, dynamic materials have also been studied with the ligands buried within the materials.[2] With the stimulation by mechanical stretching or electrical potential, the ligands will be exposed to the environment for cell adhesion. The common feature shared by these materials is that ligands are not released from the materials during the dynamic regulation of cell adhesion and the accessibility of ligands to cells is reversible. While these elegant materials are promising for broad applications, they may not be appropriate in situations where mechanical stretching or electrical potential are difficult to apply or change.

The purpose of this study was to synthesize a new dynamic hydrogel for which the cell adhesion function is reversibly controlled by the molecular reconfiguration of an encrypted ligand during the hybridization reactions (Figure 1; Supporting Information, Figure S1). The key functional units of the hydrogel for cell adhesion are encrypted nucleic acid aptamers that are covalently conjugated to the hydrogel network. As the aptamers maintain the covalent immobilization state in the hydrogels without loss or cleavage during the regulation, the cell adhesion function of the hydrogels can be dynamically and reversibly regulated. Moreover, as the aptamers will not be released from the hydrogel, the likelihood that the released free aptamers can negatively influence cell behavior is not a concern for this design of dynamic hydrogels.

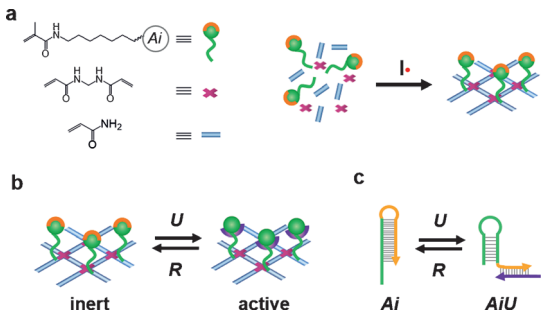

Figure 1. a) Synthesis of the hydrogel. *Ai* is the cell adhesion molecule with two functional domains, I• is the initiator. b) Illustration of the remodeling of the *Ai*-functionalized hydrogel during the hybridization reactions. The function of the hydrogel is determined by the active and inert states of *Ai*, respectively. *U* is the unblocking sequence, and *R* is the recovering sequence. c) Illustration of structural changes during the molecular reconfiguration.

The encrypted aptamer sequence has two functional domains: one is used for cell binding; the other is used for blocking the binding domain (Supporting Information, Figure S1). The cell binding domain is a short aptamer that is truncated from its parent sequence. The model aptamer used in this work is able to recognize CCRF-CEM cells through its specific interaction with the protein tyrosine kinase receptor 7.[4] The blocking domain is also an oligonucleotide that

[*] S. Li, E. R. Gaddes, Dr. N. Chen, Prof. Y. Wang
Department of Biomedical Engineering
The Pennsylvania State University
University Park, Pennsylvania 16802 (USA)
E-mail: yxwbio@engr.psu.edu

[**] We thank the Husk Institute Microscopy Facility (University Park, PA), Dr. Justin Brown, Brittany Banik, and Yike Huang for technical support. This work was supported in part by the U.S. National Science Foundation (1322332).

Supporting information for this article is available on the WWW under http://dx.doi.org/10.1002/anie.201500397.

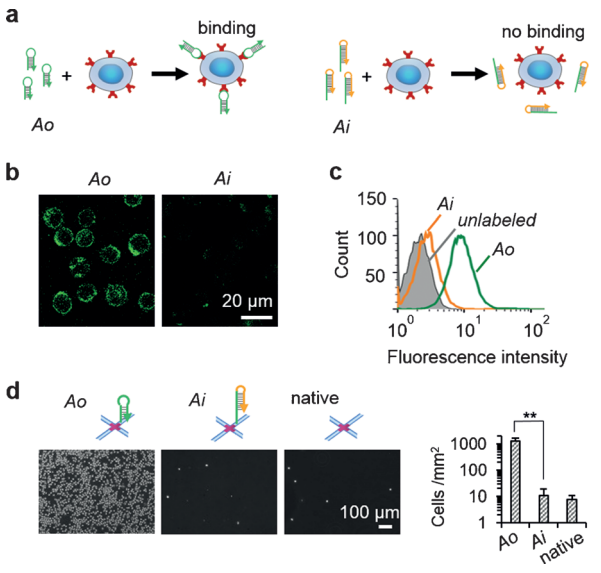

Figure 2. Design and characterization of the cell adhesion molecule. a) Illustration of cell labeling with *Ao* (left) or *Ai* (right). *Ao* is an oligonucleotide segment truncated from a full-length oligonucleotide aptamer, and *Ai* is the encrypted aptamer sequence. b) Confocal microscopy images showing the binding of FAM-labeled *Ao* or *Ai* to the cells. c) Flow cytometry histograms. d) Comparison of cell adhesion on the hydrogels with either *Ai* or *Ao*. Native: hydrogel without *Ao* or *Ai*. ** $P<0.001$, $n=3$.

partially forms intramolecular hybridization with the cell binding domain. Since the binding and blocking domains are integrated into one aptamer sequence, it was hypothesized that this intramolecular reconfiguration would lead to an inert state of the aptamer in binding to the cell (Figure 2a). To test the hypothesis, the aptamers were labeled with FAM and allowed to interact with the cells for 30 min. The microscopic images show that the cells treated by the aptamer *Ao* (that is, the binding domain without the blocking domain) exhibited strong green fluorescence whereas those treated by the aptamer *Ai* (that is, the binding domain with the blocking domain) exhibited much weaker fluorescence (Figure 2b). The flow cytometry analysis was consistent with the microscopy observation (Figure 2c).

We next chemically incorporated the aptamers into the hydrogels for the examination of cell adhesion. The results show that the cell density was approximately 10 cells per mm^2 on the *Ai*-functionalized hydrogel, which was similar to that on the native hydrogel but was two orders of magnitude less than that observed on the *Ao*-functionalized hydrogel under the same cell adhesion conditions (Figure 2d). Thus, the hydrogel with *Ai* exhibited an inert state that is inhibitive to cell adhesion. We further examined the effect of the intramolecular hybridization length on cell adhesion (Supporting Information, Figure S2). As shown in the secondary structures, while the two aptamers with a blocking domain both exhibit a stem-loop conformation, their conformations are different from that of the binding domain (that is, *Ao*) without the blocking domain. Since conformation is important to the binding function of an aptamer, the structural analysis suggests that both encrypted aptamers with the blocking domain might not bind to the cells. However, the experimental results from flow cytometry show that the cell binding capability of *Ai* with 10 intramolecular base pairs (Ai_{10}) falls in between *Ai* with 20 intramolecular base pairs (Ai_{20}) and *Ao* (Supporting Information, Figure S3). The data of cell adhesion (Supporting Information, Figure S4) are consistent with the flow cytometry analysis. At the concentration of 50 μM aptamer, the cell density of the Ai_{10}-functionalized hydrogel was about 10 times higher than that on the Ai_{20}-functionalized hydrogel but about 10 times lower than that on the *Ao*-functionalized hydrogel.

The conformations of nucleic acids are dynamic.[5] The stability of the conformations is indicated by ΔG values of the structures. A lower ΔG value suggests a more stable structural conformation. The ΔG value of the stem-loop structure of Ai_{10} is -7.83 kcal mol^{-1} whereas that of Ai_{20} is -17.31 kcal mol^{-1}. These data suggest that the blocking domain of Ai_{20} is capable of inhibiting the cell binding domain with more stability than Ai_{10}. Previous studies also demonstrate that target molecules can aid the structural change of aptamers, favoring the recovery of the functional conformation.[6] Taken together, these findings suggest that the blocking domain has to be sufficiently long to inhibit the cell binding domain. Since 20 intramolecular base pairs sufficiently inhibited the cell binding function of the aptamer, Ai_{20} was used in the following experiments.

Next, we studied whether it was possible to unblock the binding domain of *Ai* with the hypothesis that an exogenous short oligonucleotide (that is, an unblocking sequence denoted as *U*) could be used to induce the reconfiguration of *Ai* from the encrypted inert state to the active state through hybridization reaction (Figure 3a). To test this hypothesis, Ai_{20} was synthesized with a 2′-aminopurine located in the stem structure. The 2′-aminopurine exhibits stronger fluorescence when changing from a hybridized state to an unhybridized state.[7] Thus, the measurement of the fluorescence intensity would indicate the conformational change. Seven *U* sequences with different lengths were studied to unblock the

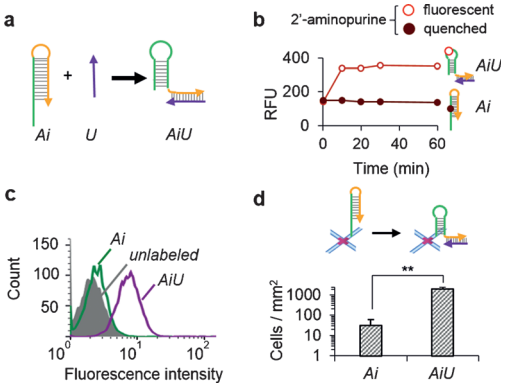

Figure 3. Examination of *U*-mediated *Ai* reconfiguration for cell adhesion. a) Illustration of *Ai* reconfiguration during the hybridization reaction. b) Reaction kinetics of *Ai* and *U*. *Ai* has a 2′-aminopurine in its stem for the evaluation of *U*-induced *Ai* reconfiguration. c) Flow cytometry histograms. d) Cell adhesion before and after the *U*-treatment. ** $P<0.001$, $n=3$. The data presented herein were produced by using Ai_{20} and U_6.

binding domain of Ai_{20} (Supporting Information, Figure S5a). As the hybridization length increased, the absolute ΔG value and the fluorescence intensity of *AiU* duplex increased (Supporting Information, Figure S5b,c). It suggests that *AiU* with longer hybridization length is more stable. The structural analysis also shows that the cell binding domain is displayed after the hybridization reaction (Supporting Information, Figure S6). Moreover, the unblocked aptamer maintained the stable unblocking conformation (Figure 3b). To further confirm whether the *U* sequence could unblock the binding domain of Ai_{20}, we used flow cytometry to examine cell labeling. The data show that Ai_{20} was able to bind to the cells in the presence of U_6 (Figure 3c). Importantly, with the treatment of U_6, the initially inert hydrogel was activated to increase cell adhesion on the hydrogel surface by two orders of magnitude (Figure 3d). Therefore, the hybridization reaction for the *U*-mediated *Ai* reconfiguration is effective for the remodeling of the hydrogel from an inert state to an active state.

A number of dynamic materials have been synthesized with a unidirectional change because of the release of ligands.[1k–m] The mechanism presented in this study is different since ligand reconfiguration does not require ligand release regardless of if the blocking domain forms intramolecular hybridization base pairs with the binding domain or if it forms intermolecular hybridization base pairs with the unblocking *U* sequence. Since *Ai* was not released from the hydrogel (Figure 2 and 3), we further hypothesized that *Ai* could return its encrypted state after the *U* sequence was separated from its blocking domain. As a result, the function of the hydrogel would re-enter the inert state, that is, inhibition of cell adhesion.

To achieve the separation of *U* from *Ai*, the variation of temperature may be used as a stimulus.[8] For instance, Kikuchi et al. developed thermosensitive poly(*N*-isopropylacrylamide) substrates for cell sheet tissue engineering.[8a] These materials allow for cell adhesion at 37 °C, whereas lowering the temperature from 37 to 20 °C causes cell detachment. However, the melting temperature of U_6 and Ai_{20} is 65 °C, which is far above the physiological temperature. Thus, while the increase of temperature can in principle lead to the separation of *U* sequence from the blocking domain, this straightforward and simple method is not suitable for the dynamic hydrogel developed in this study. To achieve the separation of *U* sequence from the blocking domain in physiological conditions, we applied a recovering sequence (*R*) to hybridize with and neutralize *U* (Figure 4a).

To aid *R* in neutralizing *U*, a 6-nt overhang was added to the 5′ end of the U_6 sequence to form a new sequence, that is, U_7 (Supporting Information, Figure S7). With this design, the intermolecular hybridization length of *R* and *U* is longer than that of *Ai* and *U*, which thermodynamically favors the *UR* hybridization in the presence of *Ai*. Since the overhang was added onto *U*, it is necessary to first examine whether the overhang would affect the hybridization reaction between *Ai* and *U*. The result from the 2′-aminopurine fluorescence analysis shows that the addition of the 6nt overhang did not affect the ability of *U* to react with *Ai* (Supporting Information, Figure S7). This result was further confirmed by flow

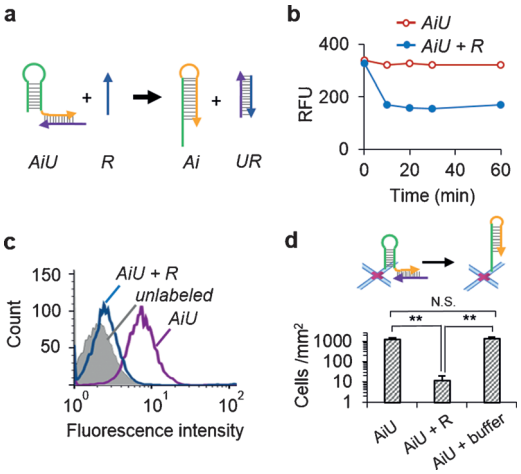

Figure 4. Examination of *Ai* reconfiguration after sequential treatments of *U* and *R* for inhibiting cell adhesion. a) Illustration of the conformational recovery of *Ai* from *AiU* during the hybridization reaction. b) Reaction kinetics of *R*-mediated separation of *U* from *Ai*. *Ai* was labeled with 2′-aminopurine. c) Flow cytometry histograms. d) Cell adhesion on the *AiU*-functionalized hydrogel before and after the buffer or *R*-treatment. ** $P<0.001$, N.S.: no significance; $n=3$. The data were produced by using Ai_{20} and U_7.

cytometry analysis showing that both *U* sequences with (U_7) and without (U_6) the overhang could unblock the cell binding domain of *Ai* (Supporting Information, Figure S8). Moreover, the AiU_7 complex was able to specifically bind to the CCRF-CEM cell line rather than the Ramos control cell line on the hydrogel surface (Supporting Information, Figure S9).

To examine the function of *R*, the *AiU* complex was treated with *R* (Supporting Information, Figure S10). The fluorescence intensity of the complex was rapidly decreased, reaching a plateau within 10 min (Figure 4b; Supporting Information, Figure S10). Since *Ai* had 2′-aminopurine, this result indicates that the *AiU* complex was separated, and that the conformation of *Ai* was changed. To examine whether *R* can change the cell binding state of *Ai*, the cells binding to the *AiU* complex were treated with *R* and examined with flow cytometry. The result shows that the *R*-treated cells exhibited virtually the same fluorescence as the untreated cells (Figure 4c), indicating that *Ai* was dissociated from the cell surface owing to the conformational change.

The function of *R* was further examined by studying the cell adhesion on the hydrogel. After the cells were attached to the hydrogels with the *AiU* complex for 0.5 h, the hydrogels were treated with the *R* solution. The *R* treatment led to the detachment of 99% of the cells from the hydrogels (Figure 4d). By contrast, the cell attachment on the hydrogels was not affected in the buffer treatment group. To understand whether cells can be detached by *R* after a longer period of cell attachment, we prolonged the cell attachment time from 0.5 to 12 h. Since the aptamer used in this study was originally selected from an aptamer library without chemical modifications,[4] the cells were incubated in medium with partially inactivated serum that was expected to have reduced nuclease activity. The images show that the cells could attach to the hydrogel surface and that the number of the cells decreased

from 6 to 12 h, which is most likely due to ligand degradation (Supporting Information, Figure S11 a,b). Importantly, the data clearly show that the cells could be effectively detached from the surface by *R* in comparison to the control buffer without *R* (Supporting Information, Figure S11 a,c). Moreover, the majority of the cells were viable (Supporting Information, Figure S11 d,e), because the entire procedure did not involve any harsh factors and the *RU* complex is not toxic (Supporting Information, Figure S12). Thus, these data show that *R* can effectively neutralize *U* during the hybridization reaction to induce the molecular reconfiguration of *Ai* from its active to inert state, thereby regulating the state of cell adhesion on the hydrogels.

We also examined cell morphology using optical and electron microscopy. While the optical microscopy images do not show any difference in cell morphology (Supporting Information, Figure S13), the SEM images show that some cells had protrusions during the first 6 h on the hydrogel whereas few cells with protrusions were observed at 12 h (Supporting Information, Figure S14). While the data suggest that this hydrogel system may find applications in the areas of cell separation or cell culture, it is important to note that chemically modified aptamers with the ability to resist nuclease degradation will be important for applications that require a long period of cell culture.

Since the hybridization reactions are able to induce the molecular reconfiguration of *Ai* but do not change the chemical bond linking *Ai* and the hydrogel, we expected that the reversible reconfiguration of *Ai* between its encrypted and active states could be sustainably repeated to inhibit and induce cell adhesion for multiple cycles by using the sequences *U* and *R*. To test the sustainable remodeling of the hydrogel, fluorophore-labeled *U* and *R* were used to sequentially treat the *Ai*-functionalized hydrogel. With the treatment of *U*, the hydrogel exhibited strong fluorescence; with the subsequent treatment of *R*, the fluorescence intensity of the hydrogel returned to the background level (Supporting Information, Figure S15). This pattern of fluorescence appearance and disappearance could be repeated for multiple times, demonstrating that *U* can repeatedly bind to *Ai* and that *R* can repeatedly neutralize *U* during the hybridization reactions. We further examined whether *U* and *R* can sequentially and repeatedly regulate cell adhesion on the hydrogel by the molecular reconfiguration of *Ai*. To avoid potential aptamer degradation, this proof-of-concept cell attachment and detachment experiment was pursued in the medium without serum. Consistent with the results shown in Figure 3 d and 4 d, the hydrogel treated with *U* allowed for cell adhesion and the subsequent treatment with *R* led to cell release (Figure 5). This pattern of inducing and inhibiting cell adhesion could be repeated during the multiple cycles of *U* and *R* treatment, demonstrating that the sequential treatment of the hydrogel with *U* and *R* could lead to the reversible reconfiguration of *Ai* for regulating the cell adhesion function of the hydrogel.

In summary, we have demonstrated a new mechanism of regulating the function of synthetic hydrogels for inducing and inhibiting cell adhesion. The regulation of adhesion and inhibition is achieved by the molecular reconfiguration of an encrypted synthetic aptamer that consists of a cell binding domain and a blocking domain. Since the encrypted aptamer is covalently conjugated to the hydrogel during the procedure of molecular reconfiguration, inhibiting and inducing cell adhesion on the hydrogel do not involve the release of free aptamers. Future work may be performed to develop dynamic hydrogels with different encrypted synthetic biomolecules for regulating the adhesion of multiple cells.

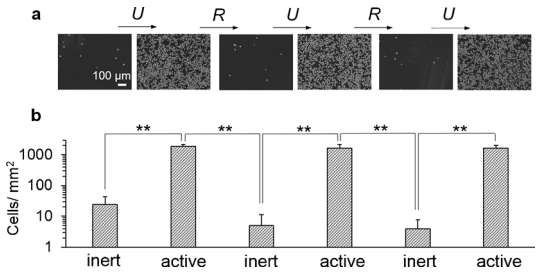

Figure 5. Multiple cycles of sequential *U* and *R* treatment of the *Ai*-functionalized hydrogel for inhibiting and inducing cell adhesion by molecular reconfiguration. a) Representative cell images. b) Quantitative analysis. U_7 and Ai_{20} were used this experiment. ** $P < 0.001$, $n = 3$.

Keywords: affinity ligands · cell adhesion · dynamic materials · hydrogels · molecular recognition

How to cite: *Angew. Chem. Int. Ed.* **2015**, *54*, 5957–5961
Angew. Chem. **2015**, *127*, 6055–6059

[1] a) M. Wirkner, J. M. Alonso, V. Maus, M. Salierno, T. T. Lee, A. J. García, A. del Campo, *Adv. Mater.* **2011**, *23*, 3907–3910; b) M. Wirkner, S. Weis, V. San Miguel, M. Álvarez, R. A. Gropeanu, M. Salierno, A. Sartoris, R. E. Unger, C. J. Kirkpatrick, A. del Campo, *ChemBioChem* **2011**, *12*, 2623–2629; c) S. Petersen, J. M. Alonso, A. Specht, P. Duodu, M. Goeldner, A. del Campo, *Angew. Chem. Int. Ed.* **2008**, *47*, 3192–3195; *Angew. Chem.* **2008**, *120*, 3236–3239; d) M. N. Yousaf, B. T. Houseman, M. Mrksich, *Angew. Chem. Int. Ed.* **2001**, *40*, 1093–1096; *Angew. Chem.* **2001**, *113*, 1127–1130; e) A. M. Kloxin, A. M. Kasko, C. N. Salinas, K. S. Anseth, *Science* **2009**, *324*, 59–63; f) J. Kim, J. Yoon, R. C. Hayward, *Nat. Mater.* **2010**, *9*, 159–164; g) N. Chen, Z. Zhang, B. Soontornworajit, J. Zhou, Y. Wang, *Biomaterials* **2012**, *33*, 1353–1362; h) Y. Wan, Y. Liu, P. B. Allen, W. Asghar, M. A. I. Mahmood, J. Tan, H. Duhon, Y.-T. Kim, A. D. Ellington, S. M. Iqbal, *Lab Chip* **2012**, *12*, 4693–4701; i) Z. Zhang, N. Chen, S. Li, M. R. Battig, Y. Wang, *J. Am. Chem. Soc.* **2012**, *134*, 15716–15719; j) H. Liu, Y. Li, K. Sun, J. Fan, P. Zhang, J. Meng, S. Wang, L. Jiang, *J. Am. Chem. Soc.* **2013**, *135*, 7603–7609; k) W. Li, J. Wang, J. Ren, X. Qu, *J. Am. Chem. Soc.* **2014**, *136*, 2248–2251; l) G. Pan, B. Guo, Y. Ma, W. Cui, F. He, B. Li, H. Yang, K. J. Shea, *J. Am. Chem. Soc.* **2014**, *136*, 6203–6206; m) T. T. Lee, J. R. García, J. I. Paez, A. Singh, E. A. Phelps, S. Weis, Z. Shafiq, A. Shekaran, A. Del Campo, A. J. García, *Nat. Mater.* **2014**, DOI: 10.1038/nmat4157.

[2] a) D. Mertz, C. Vogt, J. Hemmerlé, J. Mutterer, V. Ball, J.-C. Voegel, P. Schaaf, P. Lavalle, *Nat. Mater.* **2009**, *8*, 731–735; b) J. Davila, A. Chassepot, J. Longo, F. Boulmedais, A. Reisch, B. Frisch, F. Meyer, J.-C. Voegel, P. J. Mésini, B. Senger, et al., *J. Am. Chem. Soc.* **2012**, *134*, 83–86; c) J. Lahann, S. Mitragotri, T. Tran, H. Kaido, J. Sundaram, I. S. Choi, S. Hoffer, G. A. Somorjai, R. Langer, *Science* **2003**, *299*, 371–374; d) C. C. A. Ng, A. Magenau,

S. H. Ngalim, S. Ciampi, M. Chockalingham, J. B. Harper, K. Gaus, J. J. Gooding, *Angew. Chem. Int. Ed.* **2012**, *51*, 7706 – 7710; *Angew. Chem.* **2012**, *124*, 7826 – 7830.

[3] a) M. Mayurni, S.-I. Sumimoto, S.-I. Kanazashi, D. Hata, K. Yamaoka, Y. Higaki, T. Ishigami, K.-M. Kim, T. Heike, K. Katamura, *J. Allergy Clin. Immunol.* **1996**, *98*, 238 – 247; b) J. A. Smith, J. A. Bluestone, *Curr. Opin. Immunol.* **1997**, *9*, 648 – 654; c) M. S. Cragg, R. R. French, M. J. Glennie, *Curr. Opin. Immunol.* **1999**, *11*, 541 – 547; d) M. F. Renschler, R. R. Bhattt, W. J. Dowert, R. Levy, *Immunology* **1994**, *91*, 3623 – 3627; e) C. Henke, P. Bitterman, U. Roongta, D. Ingbar, V. Polunovsky, *Am. J. Pathol.* **1996**, *149*, 1639 – 1650; f) J. Mi, X. Zhang, P. H. Giangrande, J. O. McNamara, S. M. Nimjee, S. Sarraf-Yazdi, B. A. Sullenger, B. M. Clary, *Biochem. Biophys. Res. Commun.* **2005**, *338*, 956 – 963.

[4] D. Shangguan, Y. Li, Z. Tang, Z. C. Cao, H. W. Chen, P. Mallikaratchy, K. Sefah, C. J. Yang, W. Tan, *Proc. Natl. Acad. Sci. USA* **2006**, *103*, 11838 – 11843.

[5] a) Y. Yin, X. S. Zhao, *Acc. Chem. Res.* **2011**, *44*, 1172 – 1181; b) T. E. Ouldridge, P. Šulc, F. Romano, J. P. K. Doye, A. A. Louis, *Nucleic Acids Res.* **2013**, *41*, 8886 – 8895.

[6] a) M. N. Stojanovic, P. De Prada, D. W. Landry, *J. Am. Chem. Soc.* **2001**, *123*, 4928 – 4931; b) J. Liu, Y. Lu, *Angew. Chem. Int. Ed.* **2006**, *45*, 90 – 94; *Angew. Chem.* **2006**, *118*, 96 – 100.

[7] a) J. M. Jean, K. B. Hall, *Proc. Natl. Acad. Sci. USA* **2001**, *98*, 37 – 41; b) B. Holz, S. Klimasauskas, S. Serva, E. Weinhold, *Nucleic Acids Res.* **1998**, *26*, 1076 – 1083.

[8] a) A. Kikuchi, M. Okuhara, F. Karikusa, Y. Sakurai, T. Okano, *J. Biomater. Sci. Polym. Ed.* **1998**, *9*, 1331 – 1348; b) K. Nagase, Y. Hatakeyama, T. Shimizu, K. Matsuura, M. Yamato, N. Takeda, T. Okano, *Biomacromolecules* **2013**, *14*, 3423 – 3433; c) E. Wischerhoff, K. Uhlig, A. Lankenau, H. G. Börner, A. Laschewsky, C. Duschl, J.-F. Lutz, *Angew. Chem. Int. Ed.* **2008**, *47*, 5666 – 5668; *Angew. Chem.* **2008**, *120*, 5749 – 5752.

Received: January 15, 2015
Revised: February 26, 2015
Published online: March 25, 2015

